Anomalous intrinsic fluorescence of HCl and NaOH aqueous solutions.

Anna Maria Villa, Silvia Maria Doglia, Luca De Gioia, Luca Bertini*, Antonino Natalello*

Department of Biotechnology and Biosciences, University of Milano-Bicocca, Piazza della Scienza 2, 20126 Milan, Italy.

E-mail: luca.bertini@unimib.it; antonino.natalello@unimib.it

ABSTRACT

The unique properties of liquid water mainly arise from its hydrogen bond network. The geometry and dynamics of this network play a key role in shaping the characteristics of soft matter, from simple solutions to biosystems. Here we report an anomalous intrinsic fluorescence of HCl and NaOH aqueous solutions at room temperature, that shows important differences in the excitation and emission bands between the two solutes. From ab-initio Time-Dependent Density Functional theory modelling we propose that fluorescence emission could originate from hydrated ion species contained in transient cavities of the bulk solvent. These cavities, which are characterised by a stiff surface, could provide an environment that, trapping the excited state, suppresses the fast non-radiative decay and allows the slower radiative channel to become a possible decay pathway.

Water is a unique solvent for its importance in living organisms, where the interactions of water molecules with ions and biomolecules are at the basis of key processes like protein folding, enzymatic catalysis and energy conversion. In all these processes proton transfer and the structure of the hydration shell around biological molecules play a fundamental role.

Water ability to form a hydrogen-bonded network is at the root of many of its peculiar properties, but in spite of being one of the most studied systems, water molecular behaviour is still matter of an intense and multidisciplinary investigation.[1,2]

It is well-known that photo-excitation in the presence of solutes can populate the charge-transfer excitation bands, inducing a significant reorganization of the hydrogen-bond system through a process known as excited state hydrogen

bonding dynamics.[3] Generally, the H-bond network facilitates internal conversion (IC) processes,[4,5] however in some cases fluorescence enhancement is observed.[6,7]

In the last decade, several studies reported an anomalous fluorescence in aqueous solutions of many proteins and amyloid aggregates in absence of any aromatic residue or π systems.[8,9] Recently, it has been shown[10] that in amyloid fibrils this anomalous fluorescence is correlated with proton transfer dynamics and with a peculiar double-well shape of the ground state potential energy surface along the H-bond network, a condition that prevents the excited state decay via conic intersection and thus favors fluorescence. The sensitivity of the fibril intrinsic fluorescence to pH changes confirms that this unconventional fluorophore has properties strongly coupled to proton fluctuations. Moreover, the authors show that proton transfer in fibrils involves the compression of the hydrogen bonds, a mechanism analogous to what is seen in other H-bonded systems and, in particular, in water.[11,12,13]

The nature of the delocalised proton with double well potential has been investigated in water clusters by IR spectroscopy[14,15,16] and quantum chemistry.[17,18,19,20] Similar results have been obtained for protons in bulk water using deep inelastic neutron scattering (DINS)[21,,22,23] and simulations.[20] In particular, these neutron studies have reported the existence of an anomalous quantum state of protons when the hydrogen-bonded network of water is perturbed, either by nanoconfinement or by the presence of solutes. In this anomalous state, the H-bond potential energy surface acquires a double well character, leading to charge delocalization and proton transfer. In particular, in aqueous solutions of HCl and NaOH at concentrations between 1.6M and 3M, DINS measurements show that some protons assume a coherent bimodal distribution and that the number of protons in coherent distribution is in excess with respect to the number of the impurities added.[21] The authors interpret these data as an indication of a collective and coherent response of water network to the perturbation introduced by the solute molecules that leads to an enhanced number of delocalized protons with double well potential with respect to plain water.

These neutron studies, reporting the presence of the double-well geometry of the H-bond potential also in aqueous solution, together with the literature results showing the correlation between the double-well geometry of proton potential, proton transfer and the fluorescence of amyloid fibrils led us to hypothesize that a similar intrinsic fluorescence should be observable also in HCl and NaOH water solutions, as long as the number of delocalized protons is sufficient to give a detectable emission intensity.

In this work, we show for the first time that aqueous solutions of HCl and NaOH are indeed fluorescent in the near UV and blue range, and that the optical response induced by the two solutes is different, suggesting a substantial role of the

excess proton and hydroxide ion in shaping the spectral properties of their solutions.

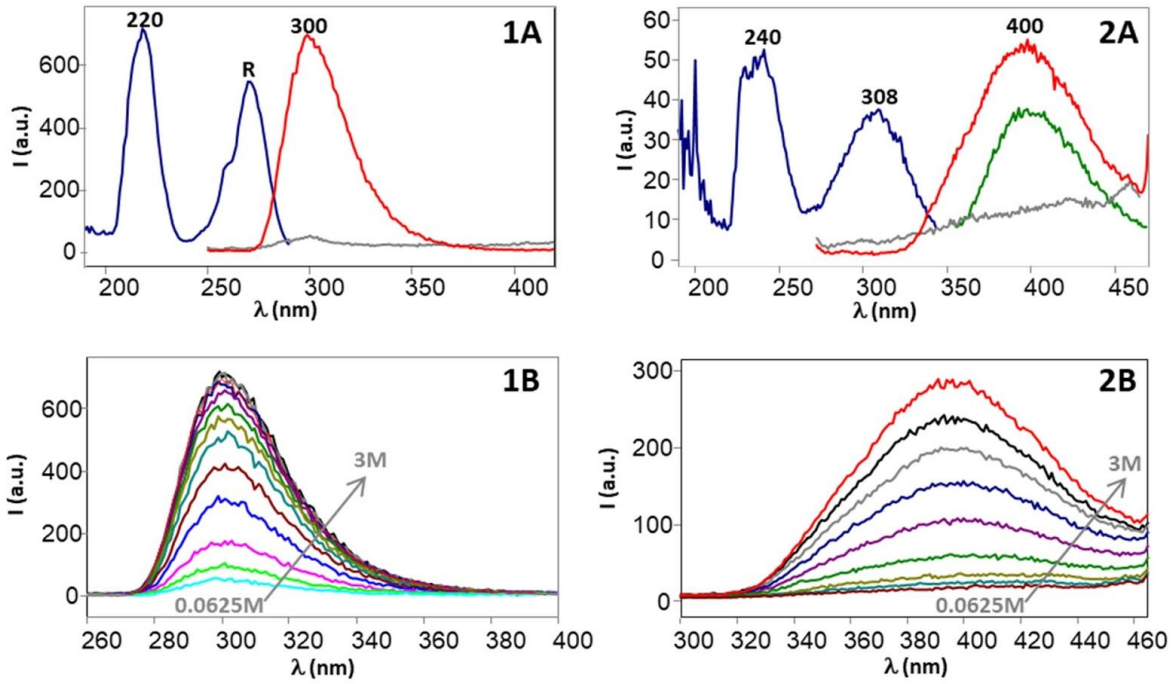

Figure 1. A) Excitation and emission spectra of 3M HCl in water. Excitation spectrum with emission centered at 300 nm (blue; R marks the Raman band) and emission spectrum with excitation centered at 220 nm (red). For comparison, the emission spectrum of 3M NaCl with excitation at 220 nm is reported (grey). B) Emission spectra of HCl in water at different concentrations from 0.0625M to 3M (excitation at 220 nm). Photomultiplier gain: 900V; excitation slit: 5 nm, emission slit: 5 nm.

Figure 2. A) Excitation and emission spectra of 3M NaOH in water. Excitation spectrum with emission centered at 400 nm (blue), emission spectra with excitation centered at 240 nm (red) and 308 nm (green). For comparison, the emission spectrum of 3M NaCl with excitation at 240 nm is reported (grey). Photomultiplier gain: 900V; excitation slit: 5 nm, emission slit: 5 nm. B) Emission spectra of NaOH in water at different concentrations from 0.0625M to 3M (excitation at 240 nm). Photomultiplier gain: 950V; excitation slit: 5 nm, emission slit: 10 nm.

Figure 1A shows that, upon excitation at 220 nm of a 3M aqueous solution of HCl, a detectable fluorescence emission is observed, with maximum intensity at 300 nm. The excitation spectrum, collected with emission centered at 300 nm,presents the higher intensity band at 220 nm and a weaker band at about 270 nm, superimposed to the Raman scattering of water. In the range between 0.065M and 3M (Fig.1B) the emission intensity increases with the solute concentration,

confirming that this unconventional fluorescence actually arise from the water-solute interaction. The absorption spectra confirmed that the 220 nm and 270 nm fluorescence excitation maxima are absorption bands of the HCl solutions (Fig. S1).

A weaker fluorescence emission was observed for the 3M aqueous solution of NaOH (Fig. 2A) compared to 3M HCl sample . Here the spectra are red shifted with respect to those of HCl, displaying two peaks in the excitation spectrum (blue) at 240 nm and 308 nm, and a single band in the emission spectra (red and green) at either 395 nm or 400 nm when the excitation was at 240 nm and at 308 nm, respectively. Also in this case, the fluorescence intensity increases with the solute concentration in the range between 0.0625M and 3M (Fig. 2B) and the presence of absorption bands at the same wavelengths of the fluorescence excitation maxima was also observed (Fig.S2).

To estimate the contribution of Na^+ and Cl^- ions to the observed fluorescence, in Fig.1A and 2A the fluorescence emission spectra of 3M NaCl aqueous solution are also reported for comparison (grey). As can be seen, the fluorescence of NaCl solution, when collected in the same conditions used for HCl and NaOH, has a much lower intensity, indicating that the major contribution to fluorescence comes from protons and OH^- ions.

The observed differences between HCl and NaOH fluorescence spectra suggest that excess proton and hydroxide ion in water induce different geometries and dynamics of the H-bond network. Noteworthy, Grisanti et al.[24] have shown that in amyloid fibrils the shrinking of the hydrogen bond, induced by small changes in the distance between the nitrogen and oxygen atoms sandwiching the proton, can produce major modifications in the potential energy surfaces of the ground and excited states. These modifications lead to significant changes in the optical properties of the system. A similar finding is reported by Hassanali et al.[11] in a computational study on liquid water, where they show that hydronium perturbs the water network in a different way compared with hydroxide ion.

Differences in the H-bond network in the investigated samples was also confirmed by FTIR analysis of HCl, NaOH and NaCl 1M solutions (Fig. S4).

To elucidate the possible mechanism of the emission process, we performed a Time-dependent Density Functional Theory (TDDFT) modelling using TURBOMOLE suite of programs[25] with B-LYP[26.27] functional and triple-ζ plus polarization split valence quality basis set.[28] (see SI for details)

This investigation on the fluorescence properties of the HCl and NaOH aqueous solution starts from the simulation of the absorption spectra of the $Cl^-(H_2O)_{54}(H_3O^+)$ and $Na^+(H_2O)_{54}(OH^-)$ model clusters at TDDFT level.

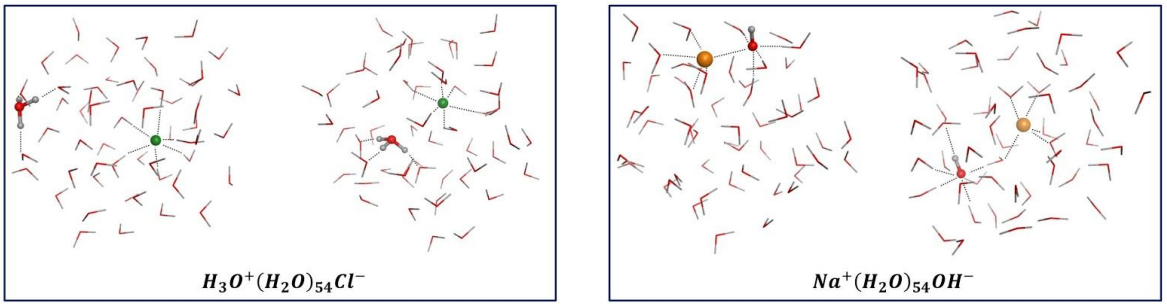

Figure 3. 1M HCl and NaOH models. For each system are sketched the most stable form with charged species on the cluster surface and the most stable form with charged species buried in the cluster (model 8 and 10 for HCl; model 2 and 4 for NaOH; see Table S1 and S2 in SI)

Here the number of water molecules considered in the model cluster (54 plus the protonated/deprotonated one, thus mimicking 1M solutions, see Fig. 3) have been established to obtain a realistic but compact model of the bulk HCl and NaOH solution in order to reproduce their absorption spectra (see SI for the details of the level of theory adopted). This implies to consider model clusters in which the ionic species are buried in the solvent although higher in energy compared with structures in which the charged ion are placed at the border of the cluster itself.[29.30.31.32] We therefore adopt the ion buried models as reference for TD-DFT computations of the excitation spectra which are reported in Fig. 4.

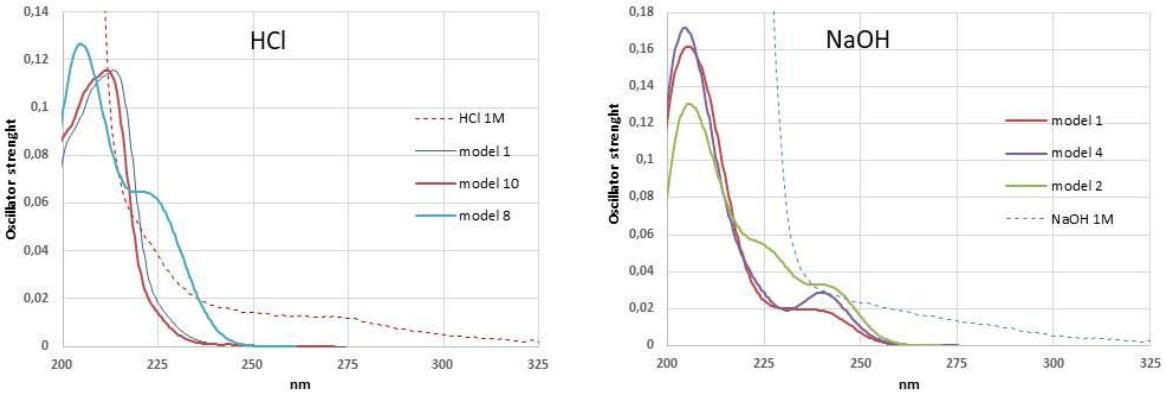

Figure 4. Computed absorption spectra for the 1M HCl and NaOH models. For each system the simulated spectrum for the most stable form (model 1 with charged species on the cluster surface) and two forms with charged species buried in the cluster are reported (model 8 and 10 for HCl; model 2 and 4 for NaOH; see Table S1 and S2 in SI)

On the basis of the occupied and unoccupied valence MO, the excited state of hydrated HCl or NaOH clusters can be classified in term of charge-transfer-to solvent band (CTTS) in which electron density is transferred from the i) a negative charged ion (Cl^- or OH^-) to an MO provided by the solvent and by the positively charged ions (H_3O^+, Na^+).[33,34,35] Regarding HCl model, the first four most intense

absorptions have Cl^-,O→H charge transfer character. The H atom primarily involved is a *dangling* one on the cluster surface which is also the closest to Cl^-. In the case of S_1, two oxygen atoms on the surface are interested but not the Cl^- anion. For NaOH, the most intense transitions involve the O → Na^+/H charge transfer (CT), where in most cases one of the oxygen atoms belongs to the hydroxide ion.

The fluorescence of the two models is first investigated by geometry relaxation of the S_1 state. These optimizations only evidence a non-radiative decay through conical intersection (CI), and exclude any fluorescence decay. This is not surprising, since the low values of the fluorescence quantum yield (QY, see SI for details) calculated from our spectra suggest that, during the vibrational cooling of the S_1 state, of the two channels – the radiative and the non-radiative one – the latter has the highest probability.

In detail, for HCl model, the S_1 potential energy surface (PES) relaxation brings first to a scramble of the H-bond network due to the O → H CT in the CTTS band and successively to an O-H bond elongation of a "*dangling*" H atoms - the H atoms on the cluster surface not fully involved in H-bonding - with the tendency of an O-H homolytic dissociation until a conical intersection with the ground state is reached. This behaviour has been already observed[36] and computations on small clusters have evidenced the formation of the H_3O radical which relaxes via CI to the ground state and dissociates. A further proof comes from a very recent simulation on the S_1 quantum dynamic of H_2O cluster that showed a mechanism in which the excited water molecule dissociates in a OH radical plus a *hot* H atom. This latter successively brings to the formation of the hydrated electron plus H_3O^+.[37] A similar result is also obtained for the NaOH model where we observe the formation of the OH radical with the concomitant dissociation of an H atom from the cluster surface at the CI to the ground state. This behaviour is in agreement with what observed for small OH^- water cluster.[35,38]

To account for fluorescence, we have been inspired by the suggestions that comes from recent literature, according to which water molecules could be able to trap the excited state due to defects in the hydrogen bond network,[39] thus preventing the non-radiative S_1 decay.[37] To simulate this latter situation, we constrained the atoms that belong to the cluster surface and carried out the same S_1 geometry optimization. This approach is in line with a recent paper in which liquid water density heterogeneities[40] are simulated by introducing, in the H-bond network, void regions surrounded by high density patches.[41] For our HCl model, we consider the ion-buried model clusters in which two or three water molecules and the hydronium ion are free to move while for the ion-buried NaOH models, there are either four or five free-to-move water molecules plus the OH^- ion. In all the cases considered, the S_1 geometry optimizations of the constrained structures converge to a local minimum with final values of the emission wavelengths that strongly depend on i) the mobility of the species inside the constrained cage ii) the

involvement in the S_1 transition of the MO that belongs to the species which are free to move.

In the case of the HCl models, the differences between emission and absorption wavelengths (Δλ) range from 3 to 671 nm (see SI), where the corresponding experimental value is 80 nm. For Δλ > 10 nm the proton hopping from the H_3O^+ ion to an unconstrained water is observed (see figure 5). Large Δλ values occur when unconstrained species have more free space in the cage to move. It is interesting that, when these HCl model constrained structures are further re-optimized on the S_0 PES, the proton does or does not return to the water molecule to which it was initially bound, depending on the relative stability of the two isomers on S_0.

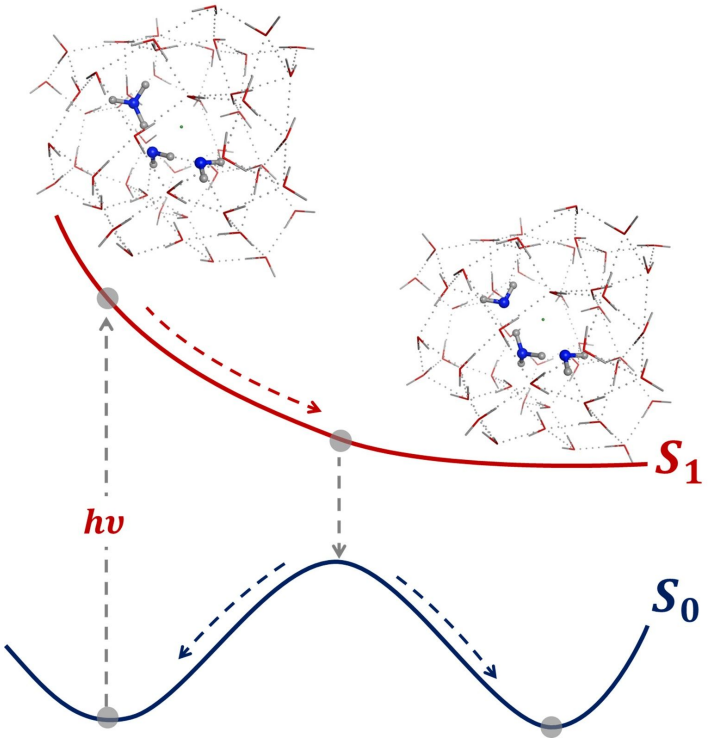

Figure 5. Scheme of the S_1 geometry optimization of the constrained most stable ion-buried 1M HCl model structure. In stick&ball are represented the unconstrained molecules at the center of the cluster. Starting from the ground state minimum geometry, upon TDDFT S_1 geometry optimization we observe the H^+ hopping to the nearest neighbor unconstrained H_2O molecule to the hydronium ion. The further optimization on the S_0 PES can converges to a new local minimum or to the initial geometry.

In the case of the NaOH buried-ion models, we observe i) the rearrangement of the OH^- H-bond network with the loss of one interaction; ii) the motion of the Na^+ ion from its S_0 equilibrium position as effect of CT. The final Δλ ranges from 5 to 529 nm (experimental Δλ equal to 92 nm). As for HCl models, small Δλ are obtained

when unconstrained moieties are not involved in the S_1 mono-electronic transition or when they have more space to move upon vibrational relaxation.

Here we would like to underline that the values obtained for the excitation energies are not an estimate of the fluorescence emission wavelengths but suggest that the hypotheses of a transient geometry of the systems, in which the vibrational relaxation is somewhat hindered preventing the non-radiative decay, could underlie the fluorescence properties of HCl and NaOH solutions. From our modelling, we can estimate a value of about 500 $Å^3$ for the volume of our clusters, which, in the distribution reported by Ansari et al.[41] belongs to the very small percentage of voids larger than 100 $Å^3$ and is in agreement with the tetrahedral-like patches observed by X ray scattering.[42] This last point suggests that the low QY of our fluorescence could be due to the low number of these fluorescence-active clusters.

In conclusion, in this paper we have reported for the first time an anomalous unexpected fluorescence emission from HCl and NaOH aqueous solutions at room temperature in the 0.0625-3M concentration range that increases with increasing solute concentration. For HCl, the emission band is centered at 300 nm (QY = 0.016), while for NaOH the emission is red-shifted to 400 nm (QY = 0.005). The comparison with the fluorescence spectrum of 3M NaCl solution suggests that the prevalent contribution to emission in HCl and NaOH solutions comes from H_3O^+ and OH^- ions. The proposed TDDFT modelling on HCl and NaOH 1M model clusters does not account for this fluorescence, but shows the usual non-radiative decay of the S_1 state through homolytic hydrogen atom dissociation. To create the conditions that lead to fluorescence emission, we have therefore constrained the atoms that belong to the cluster surface, thus preventing hydrogen abstraction and the non-radiative decay by lengthening the lifetime of the transient S_1 state enough to allow emission. We have found that this constrained vibrational cooling of S_1 not only promotes fluorescence emission, but also H^+ hopping in the HCl model, and a less specific HB network reorganization in the NaOH model. The structural motif identified by our constrained TDDFT geometry optimizations is a transient domain in the bulk solvent with a relatively rigid surface that delimitates a region containing the ion species and a few water molecules. Inside these cavities, the H-bond network connecting water molecules and ions is more flexible than that of the surface, but not enough to allow hydrogen abstraction.

Our data, together with TDDFT modelling, suggest that the unexpected fluorescence observed in HCl and NaOH aqueous solutions could arise from the transient formation of local mesoscopic domains, in which a particular and more rigid H-bonding network is established. In these domains, the CTTS excited state energy is dissipated by radiative transitions, mimicking a fluorophore with spectral characteristics that depend upon the added solute. This intriguing property of water solutions challenges the current view of the H-bond network architecture and

dynamics in liquids, and hopefully opens new perspectives in the study of proton transfer in CTTS phenomena.

REFERENCES

(1) Gallo, P.; Amann-Winkel, K.; Angell, C. A.; Anisimov, M. A.; Caupin, F.; Chakravarty, C.; Lascaris, E.; Loerting, T.; Panagiotopoulos, A. Z.; Russo, J.; et al. Water: A Tale of Two Liquids. *Chem. Rev.* **2016**, *116* (13), 7463–7500.

(2) Agmon, N.; Bakker, H. J.; Campen, R. K.; Henchman, R. H.; Pohl, P.; Roke, S.; Thämer, M.; Hassanali, A. Protons and Hydroxide Ions in Aqueous Systems. *Chem. Rev.* **2016**, *116* (13), 7642–7672.

(3) Zhao, G.-J.; Han, K.-L. Hydrogen Bonding in the Electronic Excited State. *Acc. Chem. Res.* **2011**, *45* (3), 404–413.

(4) Oshima, J.; Yoshihara, T.; Tobita, S. Water-Induced Fluorescence Quenching of Mono- and Dicyanoanilines. *Chem. Phys. Lett.* **2006**, *423* (4-6), 306–311.

(5) Barman, N.; Singha, D.; Sahu, K. Fluorescence Quenching of Hydrogen-Bonded Coumarin 102-Phenol Complex: Effect of Excited-State Hydrogen Bonding Strength. *J. Phys. Chem. A* **2013**, *117* (19), 3945–3953.

(6) Okada, Y.; Sugai, M.; Chiba, K. Hydrogen-Bonding-Induced Fluorescence: Water-Soluble and Polarity-Independent Solvatochromic Fluorophores. *J. Org. Chem.* **2016**, *81* (22), 10922–10929.

(7) Su, Y.; Li, K.; Yu, X. Theoretical Studies on the Fluorescence Enhancement of Benzaldehydes by Intermolecular Hydrogen Bonding. *J. Phys. Chem. B* **2019**, *123* (4), 884–890.

(8) Chan, F. T. S.; Kaminski Schierle, G. S.; Kumita, J. R.; Bertoncini, C. W.; Dobson, C. M.; Kaminski, C. F. Protein Amyloids Develop an Intrinsic Fluorescence Signature during Aggregation. *Analyst* **2013**, *138* (7), 2156.

(9) del Mercato, L. L.; Pompa, P. P.; Maruccio, G.; Torre, A. D.; Sabella, S.; Tamburro, A. M.; Cingolani, R.; Rinaldi, R. Charge Transport and Intrinsic Fluorescence in Amyloid-like Fibrils. *Proceedings of the National Academy of Sciences* **2007**, *104* (46), 18019–18024.

(10) Pinotsi, D.; Grisanti, L.; Mahou, P.; Gebauer, R.; Kaminski, C. F.; Hassanali, A.; Kaminski Schierle, G. S. Proton Transfer and Structure-Specific Fluorescence in Hydrogen Bond-Rich Protein Structures. *J. Am. Chem. Soc.* **2016**, *138* (9), 3046–3057.

(11) Hassanali, A.; Giberti, F.; Cuny, J.; Kühne, T. D.; Parrinello, M. Proton Transfer through the Water Gossamer. *Proceedings of the National Academy of Sciences* **2013**, *110* (34), 13723–13728.

(12) Ceriotti, M.; Cuny, J.; Parrinello, M.; Manolopoulos, D. E. Nuclear Quantum Effects and Hydrogen Bond Fluctuations in Water. *Proceedings of the National Academy of Sciences* **2013**, *110* (39), 15591–15596.

(13) Chen, M.; Zheng, L.; Santra, B.; Ko, H.-Y.; DiStasio, R. A., Jr; Klein, M. L.; Car, R.; Wu, X. Hydroxide Diffuses Slower than Hydronium in Water Because Its Solvated Structure Inhibits Correlated Proton Transfer. *Nat. Chem.* **2018**, *10* (4), 413–419.

(14) Thamer, M.; De Marco, L.; Ramasesha, K.; Mandal, A.; Tokmakoff, A. Ultrafast 2D IR Spectroscopy of the Excess Proton in Liquid Water. *Science* **2015**, *350* (6256), 78–82.

(15) Dahms, F.; Fingerhut, B. P.; Nibbering, E. T. J.; Pines, E.; Elsaesser, T. Large-Amplitude Transfer Motion of Hydrated Excess Protons Mapped by Ultrafast 2D IR Spectroscopy. *Science* **2017**, *357* (6350), 491–495.
(16) Fagiani, M. R.; Knorke, H.; Esser, T. K.; Heine, N.; Wolke, C. T.; Gewinner, S.; Schöllkopf, W.; Gaigeot, M.-P.; Spezia, R.; Johnson, M. A.; et al. Gas Phase Vibrational Spectroscopy of the Protonated Water Pentamer: The Role of Isomers and Nuclear Quantum Effects. *Phys. Chem. Chem. Phys.* **2016**, *18* (38), 26743–26754.
(17) Mella, M.; Clary, D. C. Zero Temperature Quantum Properties of Small Protonated Water Clusters (H2O)nH (n=1–5). *J. Chem. Phys.* **2003**, *119* (19), 10048–10062.
(18) Goyal, P.; Elstner, M.; Cui, Q. Application of the SCC-DFTB Method to Neutral and Protonated Water Clusters and Bulk Water. *J. Phys. Chem. B* **2011**, *115* (20), 6790–6805.
(19) Kale, S.; Herzfeld, J. Proton Defect Solvation and Dynamics in Aqueous Acid and Base. *Angew. Chem. Int. Ed Engl.* **2012**, *51* (44), 11029–11032.
(20) Kondati Natarajan, S.; Morawietz, T.; Behler, J. Representing the Potential-Energy Surface of Protonated Water Clusters by High-Dimensional Neural Network Potentials. *Phys. Chem. Chem. Phys.* **2015**, *17* (13), 8356–8371.
(21) Reiter, G.; Mayers, J.; Abdul-Redah, T. Coherence in the Momentum Distribution of Protons in Dilute Acids and Bases. *Physica B Condens. Matter* **2006**, *385-386*, 234–235.
(22) Senesi, R.; Pietropaolo, A.; Bocedi, A.; Pagnotta, S. E.; Bruni, F. Proton Momentum Distribution in a Protein Hydration Shell. *Phys. Rev. Lett.* **2007**, *98* (13). https://doi.org/10.1103/physrevlett.98.138102.
(23) Reiter, G. F.; Kolesnikov, A. I.; Paddison, S. J.; Platzman, P. M.; Moravsky, A. P.; Adams, M. A.; Mayers, J. Evidence for an Anomalous Quantum State of Protons in Nanoconfined Water. *Phys. Rev. B: Condens. Matter Mater. Phys.* **2012**, *85* (4). https://doi.org/10.1103/physrevb.85.045403.
(24) Grisanti, L.; Pinotsi, D.; Gebauer, R.; Kaminski Schierle, G. S.; Hassanali, A. A. A Computational Study on How Structure Influences the Optical Properties in Model Crystal Structures of Amyloid Fibrils. *Phys. Chem. Chem. Phys.* **2017**, *19* (5), 4030–4040.
(25) Ahlrichs, R.; Bär, M.; Häser, M.; Horn, H.; Kölmel, C. Electronic Structure Calculations on Workstation Computers: The Program System Turbomole. *Chem. Phys. Lett.* **1989**, *162* (3), 165–169.
(26) Perdew, J. P.; Wang, Y. Accurate and Simple Analytic Representation of the Electron-Gas Correlation Energy. *Phys. Rev. B Condens. Matter* **1992**, *45* (23), 13244–13249.
(27) Becke, A. D. Density-Functional Exchange-Energy Approximation with Correct Asymptotic Behavior. *Phys. Rev. A Gen. Phys.* **1988**, *38* (6), 3098–3100.
(28) Schäfer, A.; Huber, C.; Ahlrichs, R. Fully Optimized Contracted Gaussian Basis Sets of Triple Zeta Valence Quality for Atoms Li to Kr. *J. Chem. Phys.* **1994**, *100* (8), 5829–5835.
(29) Hodges, M. P.; Wales, D. J. Global Minima of Protonated Water Clusters. *Chem. Phys. Lett.* **2000**, *324* (4), 279–288.
(30) Crespo, Y.; Hassanali, A. Unveiling the Janus-Like Properties of OH(-). *J. Phys.*

Chem. Lett. **2015**, *6* (2), 272–278.
(31) Choi, T. H.; Liang, R.; Maupin, C. M.; Voth, G. A. Application of the SCC-DFTB Method to Hydroxide Water Clusters and Aqueous Hydroxide Solutions. *J. Phys. Chem. B* **2013**, *117* (17), 5165–5179.
(32) Roy, D. R. Theoretical Study of Microscopic Solvation of NaOH in Water: NaOH(H2O)n, n=1–10. *Chem. Phys.* **2012**, *407*, 92–96.
(33) Sobolewski, A. L.; Domcke, W. Photochemistry of HCl(H2O)4: Cluster Model of the Photodetachment of the Chloride Anion in Water. *ChemInform* **2003**, *34* (19). https://doi.org/10.1002/chin.200319014.
(34) Sobolewski, A. L.; Domcke, W. Photochemistry of Mcl(H2O)4, M = H, Li, Na Clusters: Finite-Size Models of the Photodetachment of the Chloride Anion in Salt Solutions. *Phys. Chem. Chem. Phys.* **2005**, *7* (5), 970–974.
(35) Zanuttini, D.; Gervais, B. Ground and Excited States Of OH(-)(H2O)n Clusters. *J. Phys. Chem. A* **2015**, *119* (29), 8188–8201.
(36) Ončák, M.; Slavíček, P.; Fárník, M.; Buck, U. Photochemistry of Hydrogen Halides on Water Clusters: Simulations of Electronic Spectra and Photodynamics, and Comparison with Photodissociation Experiments. *J. Phys. Chem. A* **2011**, *115* (23), 6155–6168.
(37) Ziaei, V.; Bredow, T. Qualitative Assessment of Ultra-Fast Non-Grotthuss Proton Dynamics in S1 Excited State of Liquid H2O from Ab Initio Time-Dependent Density Functional Theory. *Eur. Phys. J. B* **2017**, *90* (11). https://doi.org/10.1140/epjb/e2017-80329-7.
(38) Dubosq, C.; Zanuttini, D.; Gervais, B. RASPT2 Analysis of the F–(H2O)n=1–7 and OH–(H2O)n=1–7 CTTS States. *J. Phys. Chem. A* **2018**, *122* (35), 7033–7041.
(39) Gasparotto, P.; Hassanali, A. A.; Ceriotti, M. Probing Defects and Correlations in the Hydrogen-Bond Network of Ab Initio Water. *J. Chem. Theory Comput.* **2016**, *12* (4), 1953–1964.
(40) Messina, F.; Bräm, O.; Cannizzo, A.; Chergui, M. Real-Time Observation of the Charge Transfer to Solvent Dynamics. *Nat. Commun.* **2013**, *4*, 2119.
(41) Ansari, N.; Dandekar, R.; Caravati, S.; Sosso, G. C.; Hassanali, A. High and Low Density Patches in Simulated Liquid Water. *J. Chem. Phys.* **2018**, *149* (20), 204507.
(42) Huang, C.; Wikfeldt, K. T.; Tokushima, T.; Nordlund, D.; Harada, Y.; Bergmann, U.; Niebuhr, M.; Weiss, T. M.; Horikawa, Y.; Leetmaa, M.; et al. The Inhomogeneous Structure of Water at Ambient Conditions. *Proceedings of the National Academy of Sciences*. 2009, pp 15214–15218. https://doi.org/10.1073/pnas.0904743106.